

ALLOWANCE FOR THE UNSTEADINESS OF THE FLOW IN DETERMINING THE CRITICAL CAVITATION NUMBER FOR MARINE PROPELLERS

É. L. Amromin, A. V. Vasil'ev, and E. N. Syrkin

UDC 532.528

A method of estimating the critical cavitation number for marine propeller blades is proposed. This method is based on the reduction of the three-dimensional unsteady problem to the three-dimensional steady problem and a series of two-dimensional unsteady problems.

One of the principal characteristics of marine propellers is the critical cavitation number σ_i , since it determines the speed at which cavitation bursts, accompanied by their well-known negative effects, occur on or near the propeller blades. The lack of satisfactory methods of theoretically determining the critical cavitation number has led to the long-standing use in engineering practice of a method based on the adaptation to natural conditions of the results of model experiments involving the visual recording of the onset of cavitation (so-called quasiacoustic testing, which gives the dependence of σ_i on $J = V_a/nD$, where D is the diameter of the propeller, n is its speed, and V_a is the approach-stream velocity).

When this approach is adopted, two main difficulties are encountered. The first is associated with the presence of strong scale effects, the second with the difference in the operating conditions of a model propeller in a steady water tunnel flow and a real propeller in an unsteady natural flow when the velocities vary during each revolution even when $n = \text{const}$, because the blades cut the boundary layer or wake of the hull (see, for example, the illustrations on pp. 225 and 515 of [1]).

In order to overcome these difficulties, it is usual to make three assumptions [1] in explicit or implicit form: 1) for the same J the cavitation modes developing on the propeller and the model are identical; 2) the critical cavitation numbers are proportional to a power of the Reynolds number $\sigma_i \sim \text{Re}^m$, the parameter m being determined by the cavitation mode and being independent of the blade geometry; 3) the quasisteady approach is valid, i.e., the values of σ_i can be determined for a steady uniform flow over the propeller whose velocity is equal to the extremal of the instantaneous values of the velocity of the unsteady flow impinging on the blades.

However, these assumptions have proved to be applicable only to propellers with an optimum (in terms of its efficiency) law of load distribution along the blade radius. At the same time, engineering practice has led to the unloading of the end sections and the error of the above-mentioned empirical approach has increased unacceptably: even the assumption concerning the correspondence of the cavitation modes of the model and the real propeller is no longer satisfied; under natural conditions the blades begin to cavitate and under model conditions their tip vortices.

The calculation methods [2] have so far made it possible to overcome only the difficulties associated with the scale effects attributable to viscosity and surface tension. It is difficult to use the Fourier series apparatus [3], traditional in propeller theory, for investigating unsteady effects, since the real approach streams are very complex: an idea of this can be gained from Fig. 1, the chain curves at the top of which represent the results of measuring the axial velocity component of the approach stream at the after end of a ship model for relative radii r whose decoupled values are indicated by the numbers adjacent to the curves; θ is the polar angle in the cylindrical coordinate system moving with the propeller hub, and V_a has been divided by the ship's speed. In order to describe such flows it is necessary to retain many harmonics, the volume of computation increasing with their number, and it becomes very complicated to use the above-mentioned approach to construct the blade pressure distributions.

Below, it is shown that there exists a possibility of estimating the effect of the unsteadiness of the flow impinging on the blades on the values of σ_i by slightly complicating the procedure for calculating the pressure on the blades as compared with [2]: it is sufficient to separate the three-dimensional and unsteady effects. For not very broad zones of sharp variation of V_a the lattice and finite-span effects will vary only slightly during a revolution, making an almost constant contribution to the nonuniformity of the flow impinging on the profile of the cylindrical section of the blade. Then the changes in the dimensionless pressure coefficient C_p can be found from the solution of the plane potential problem for that profile in an oncoming flow whose unsteadiness is associated only with the oscillations of the velocity component normal to the chord.

As in [2], the pressure thus determined is used for calculating the shape of the cavities for given values of the Reynolds

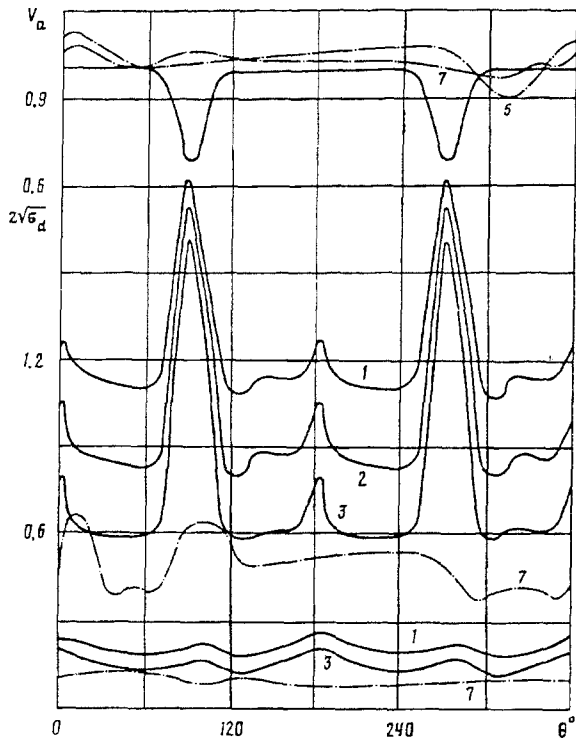


Fig 1

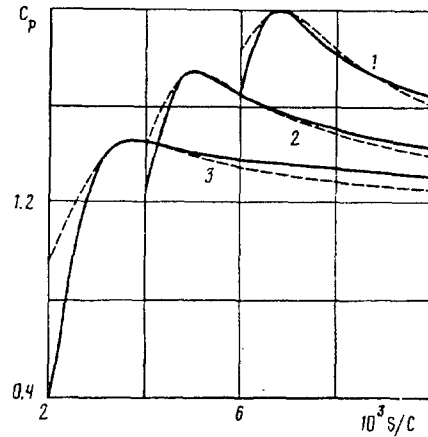


Fig 2

Re and Weber We numbers; but here it is necessary to determine only the greatest of the values of the cavitation number $\sigma = 2p\rho^{-1}(\pi nD)^{-2}$ at which a cavity can exist anywhere on the blade for fixed values of D , n and the pressure difference between the undisturbed flow and the cavity $p(r)$. The quantity πnD is used in constructing the cavitation number σ because it is precisely the rate of rotation of the end section of the blades that best characterizes the dynamic head of the flow passing over them.

Since it is proposed to investigate the initial stages of cavitation, characterized by relatively small and thin cavities which do not seriously modify the pressure on the blades as compared with cavitationless flow at the same values of n and D and the same V_a , we can divide the problem into two parts as described in [2]. The first part involves seeking the pressure diagram for cavitationless flow over the blades, complicated in this case by the need to take into account the unsteadiness of the flow, while the second involves calculating the shape of the cavities for known values of Re and We. Both parts of the problem are solved by means of approximate methods. The results of this approach are compared with those of the quasisteady approach and the possibilities of the latter in both calculations and experiments are analyzed.

1. As usual in propeller theory [1, 3], it is assumed that the propeller introduces into the flow only potential disturbances and that for any cylindrical blade section for a given value of $J = V^*/nD$ and uniform flow conditions the resulting velocities can be calculated by the same methods of three-dimensional potential theory as in [1–3]. Then the two-dimensional problem is solved in the plane of that section and the oncoming flow potential is found in the form $\Phi^* = x + ay + bxy$. The coefficients of this sum are so chosen that in this plane flow the profile has the same lift coefficient C_y and the same minimum C_p as a blade in a three-dimensional uniform flow.

As may be seen from Fig. 2, in such a two-dimensional potential flow (continuous curves) the C_p distribution near the pressure minimum on a typical propeller profile is similar to that realized at that point on the blade in a three-dimensional flow (broken curves); as abscissa we use the arc s^* , divided by the chord length C , which is counted off from the forward stagnation point. Curves 1–3 relate to the values $J = 0.51, 0.6, \text{ and } 0.7$ and $C_y = 0.23, 0.21, \text{ and } 0.17$; to these values there correspond the coefficients $a = 0.164, 0.143, \text{ and } 0.133$ and $b = -0.199, -0.175, \text{ and } -0.173$. The potential Φ^* was determined near the profile using these coefficients, and it can be continued to infinity, for example, with a discontinuity in the derivatives but with conservation of the value of C_y .

For small C_y , for which the extremum of C_p is less sharp, its positions in the plane flow thus constructed and in the three-dimensional flow around the blade cannot be made to coincide so accurately as in Fig. 2 and the displacement may be of the order of one hundredth of the chord; however, under experimental conditions the cavities typical of these regimes are attached to the blade with approximately the same scatter and consequently the displacement should not have much significance in the problem in question.

After finding the coefficients in the expression for Φ^* , by analogy with the approaches used in propeller theory [1, 3], we determine the C_p diagrams by calculating the unsteady flow over the blades in a two-dimensional nonuniform oncoming flow whose components can be represented in the form:

$$U_0 = 1 + by, \quad V_0 = a + bx + \frac{V_a - V^*}{[V^{*2} + (\pi nrD)^2]^{0.5}} \quad (1.1)$$

Here, V^* is the average value of V_a . In (1.1) only V_a depends on time, this function — the result of measurements made in the ship's boundary layer — not being harmonic. In order to formulate the problem of finding the C_p on the profile as a boundary-value problem of potential theory it is necessary to approximate the velocities (1.1) by means of harmonic functions. No attempt should be made to reconstruct the potential in the plane of the profile x, y from two arbitrary components of the velocity on the profile or its chord, since such attempts were shown to be incorrect as long ago as 1922 [4].

The approximating potential can be constructed by means of dipoles distributed along the chord, whose axes are orthogonal to the chord and whose intensities depend only on the distribution of the instantaneous values of V_a along it. The potential oncoming flow thus constructed is almost three-dimensional around relatively thin propeller profiles, since the first of conditions (1.1) is infringed only by an amount of the order of $(y/C)^2$. Accordingly, the calculation of the unsteady flow over the profile will be carried out by means of a generalization of the vortex method [5] and reduces to the solution of a system of integral equations in the intensities of the attached vortices γ , distributed over the surface of the profile S , and the free vortices Γ shed from its trailing edge and traveling in the unsteady flow along a departing ray at the velocity indicated in the denominator of the fraction in expression (1.1):

$$\frac{\gamma}{2} + \frac{1}{2\pi} \int_{(S)} \gamma \frac{\cos(N, R)}{R} dS + \sum_i \Gamma_i \frac{\partial \psi}{\partial N} = N_y U_0 - N_x V_0 \quad (1.2)$$

$$\int_S \gamma dS + \sum_i \Gamma_i = \text{const} \quad (1.3)$$

$$\gamma \{1 - 2\varepsilon\} = 2^{\beta/(2\pi-\beta)\gamma} \{1 - \varepsilon\} \quad (1.4)$$

Here, R is the distance from the arbitrary point to the check point on S ; $N = \{N_x, N_y\}$ is the outward normal to S , β is the angle of taper of the trailing edge, $0 < \varepsilon \ll 1$, the chord length is taken equal to unity, and ψ is the free vortex stream function.

At each check point on the profile we consider Eq. (1.2), which is equivalent to its impermeability condition. Condition (1.3) is the law of conservation of total vorticity in the two-dimensional flow, and expression (1.4), a consequence of the Joukowski—Chaplygin condition, is the asymptotic law for the velocity as the trailing edge is approached [6].

After solving (1.2)—(1.4), we calculate the pressure on S at each moment of time t by means of the Lagrange—Cauchy integral. It should be noted that, although it leads to certain errors, the assumption that the free vortices depart along the above-mentioned ray makes it possible to reduce the computation volume by not less than an order, since it proved to be possible in the linear algebraic system of the form $A\gamma + B\Gamma = f(t)$ substituted in calculating (1.2)—(1.4) to calculate the matrices A and B once only and to make only one calculation for the matrices for determining the contribution of the vortices to $\partial\Phi/\partial t$; moreover, near the leading edge, where cavitation begins, these errors are only small.

Thus, the solution of the very complex three-dimensional unsteady problem reduces to the solution of the three-dimensional steady problem and a series of two-dimensional unsteady problems of approximately the same difficulty as the steady problem [5]. In the method proposed all the unsteady effects relating to the variation of the pressure on the blade are analyzed in the two-dimensional approximation. At the same time, the traditional method of taking into account the effect of oncoming flow nonuniformity by constructing at each moment of time a new "equivalent profile" with its maximum curvature modified in accordance with the Morgan correction [3] is impractical because of the need to recalculate the matrices A and B for each t , but even more important is the fact that the separate allowance for the effect of the profile thickness and curvature distributions made in the traditional approach is justified only for small induced velocities, i.e., when $|C_p| \ll 1$. However, in seeking the critical cavitation number the parts of the profile on which C_p is of the order of unity are the most important.

Some examples of the calculation of the characteristics of unsteady flows are presented in Fig. 1. In the middle of the figure we have plotted the dependence on θ of the coefficient σ_D at the point of maximum underpressure on the suction side of the profile previously used in constructing Fig. 2 ($-\sigma_D$ is the minimum value of σ calculated in an ideal fluid for which it is identified with the critical cavitation number), while at the bottom of the figure we have plotted the function $C_y(\theta)$. The $V_a(\theta)$ distribution in the wake of the airfoil used in the laboratory experiments to create an unsteady oncoming flow is represented by the continuous curve at the top of Fig. 1. The dependence of C_y and σ_D on θ for a blade in this wake is given for the same

values of J and with the same numbering as the results presented in Fig. 2.

For the oncoming flow characteristics presented in Fig. 1 the analogous curves for a ship's hull are given for $J=0.9$ and numbered 7. The azimuthal angle θ in Fig. 1 is proportional to time. When the leading edge of the profile crosses the zones of minimum V_a in the wake of the airfoil at $\theta=90$ and 270° , σ_D peaks sharply. Smaller peaks and a maximum increase in C_y are observed when these zones are crossed by the trailing edge (for the given parameter rD/c at $\theta=3$ and 183°). Clearly, in the unsteady flow the pressure minimum is not determined by the instantaneous value of the lift force.

A comparison [7] of the values of C_p calculated by the method described and the experimental values for a profile in a pulsating flow indicates that the accuracy of the calculations is satisfactory.

2. Here, as in [2], the general scheme for calculating the initial stages of propeller blade cavitation is based on the theory described in [8] and below only those features of the calculations associated with the unsteadiness of the flow and the need to find the maximum possible value of σ are discussed. It should be emphasized that in [8] the effect of viscosity on cavitation was investigated, only as the relation between the dimensions and conditions of existence of the cavities and the displacement thickness δ^* and momentum thickness δ^{**} of the boundary layer; integral methods were used for calculating these thicknesses.

For unsteady flows these methods would have to be modified and a new term $\partial[(1-H_1)U\delta^*]/\partial t - \delta^*\partial U/\partial t$, where H_1 is the ratio of the thickness of the boundary layer to δ^* and U is the velocity at its outer edge, should appear on the left side of the Kármán equation, while the equation itself should be transformed from an ordinary into a partial differential equation. However, as a rule, the initial stages of cavitation develop in a very small neighborhood of the leading edge of the profile of length $l \ll C$ and if the width of the region of nonuniformity $z \lesssim C$, then, since for $t \sim z/U$ we have $U \sim Dnr$, $\partial U^2/\partial x \sim U^2/l$, $\partial(u\delta^*)/\partial t \sim \delta^*U^2/z$, it turns out that the new term in the Kármán equation is negligibly smaller than the rest. Therefore, by calculating C_p on the boundaries of the displacement body and the cavity by means of the Lagrange—Cauchy and not the Bernoulli integral, we need not otherwise correct the procedure for calculating the boundary layer characteristics as compared with [8].

The problem of finding $\max \sigma$ involves the question of what to take as the onset of cavitation. Whatever the flow characteristics there are microbubbles drifting in the water or adsorbed on the body. The development of these cavitation nuclei into cavities visible to the naked eye usually coincides with an intensification of the hydrodynamic noise or lags slightly behind it and, for practical purposes, could be regarded as the onset of cavitation. Since the corresponding cavitation numbers are random quantities, for determining their mathematical expectation experimenters have long been recording not the appearance but the disappearance of cavities on the body with slow increase in the pressure in the oncoming flow [9] or the cavitation disappearance number (which often differs little from the corresponding number for the appearance of cavitation [10]). In accordance with this experimental practice, as in [8, 11], as σ_i we have taken the maximum value of the cavitation number at which a cavity attached to the body can exist. The effect of the gas content of the flow is not taken into account in the calculations, as justified for propellers in [2].

Finding σ_i is a multistage procedure: after determining the C_p on the profile in the unsteady flow we sort out the pairs of abscissas of the beginning and end of the cavities and, as a result of solving the quasiplane quasilinear problem [8] first find the corresponding values of σ and We for a given Re and construct nomograms, which are then used for interpolating the dependence of the cavity length L on the cavitation number.

In Fig. 3 we have plotted typical dependences of L on $\sigma^{0.5}$ in a uniform oncoming flow for various J , using the same numbering of the curves as in Fig. 2. Here, in the top right-hand corner above the axis of abscissas to a dimensional scale we have shown in greater detail the parts of the same curves corresponding to very short cavities. All these results relate to $n=20 \text{ sec}^{-1}$ and to a propeller model with $D=0.35 \text{ m}$.

The curves at the top of Fig. 3 clearly demonstrate the presence of a maximum of $\sigma(L)$ due to the effect of capillarity; they confirm the weak influence on the characteristics of very short cavities of the significant discrepancy between the two-dimensional and three-dimensional pressure diagrams on the interval between the leading edge of the profile and the zone of minimum C_p . This was to be expected since, even for full-scale propellers, the boundary layer there is still laminar, while in the underpressure zone its displacement thickness depends more strongly on the local pressure than on the previous history of the flow. Finally, the maximum of $\sigma(L)$ can correspond only to small L , for which the recording of the cavity by visualization, as, for example, in [10], is improbable and in this lies the principal reason why the visual recording of cavitation often lags behind its acoustic detection.

3. The results of the approximate calculations must be compared with a control experiment. Below, as such an experiment we will use the measurements made for a propeller in the airfoil wake represented in Fig. 1. The comparison is made difficult by the fact that under laboratory conditions a moderately loaded propeller with $D=0.35 \text{ m}$, designed for $J=0.88$, begins to produce cavitation at much smaller J , i.e., at high loads for which the linear theory [1, 3] already gives significant errors in calculating C_p . Therefore, in Fig. 4 we have compared the values of R_i — the square root of the ratio of the critical cavitation numbers in the nonuniform and uniform flows: the chain curve corresponds to the calculations for an ideal fluid, the continuous curve to the calculations for the experimental conditions in accordance with the theory described, and the points to the

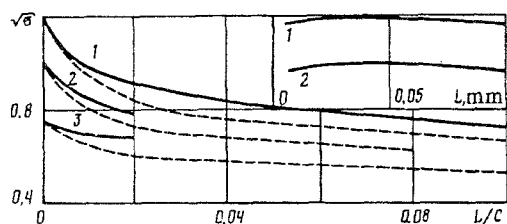


Fig 3

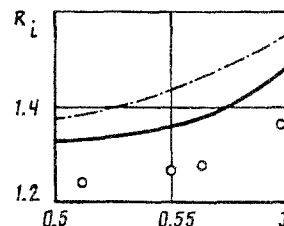


Fig 4

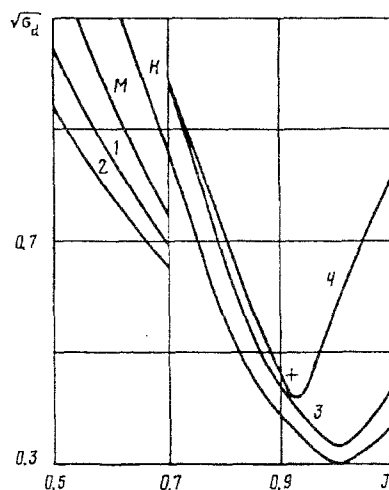


Fig 5

experimental data.

While the general trend is preserved, as was to be expected, the calculated value of R_i is higher than the observed value, since it is more difficult to visualize short cavities in a pulsating nonuniform flow than in a steady uniform flow. The satisfactory agreement between calculation and experiment makes it possible to employ the theory described for analyzing the quasisteady approach to the prediction of σ_i .

This approach is based on the use of cavitation diagrams of the type reproduced in Fig. 5. The curve H represents the calculated function $\sigma_i(J)$ for the propeller with $D=3.7$ m in a uniform flow, and the curve M that for a model propeller with $D=0.35$ m in the same flow. Precisely such curves are used in the quasisteady approach, in which the extrema of J are first found from the $V_a(\theta)$ curve, after which the values of the critical cavitation number in the steady oncoming flow are found from these J . The results of these quasisteady extrapolations for the oncoming flow represented by curve 7 in Fig. 1 are illustrated by curve 3 in Fig. 5. In the experimental construction of the diagrams at least three types of errors are present.

The first error is attributable to the scale effects and is confirmed by the difference between the M and H curves, which depends, in particular, on the shape of the blades and cannot be transferred from one object to another. The second is associated with the difficulty of recording small cavities: curves 1 and 2 in Fig. 5 represent the calculated function $\sigma(J)$ for cavities 1 and 2 mm long, respectively, and it is clear how much σ_i can be underestimated as a result of a certain delay in recording the cavities. Therefore with the above-mentioned empirical approach to predicting σ_i one should in fact operate not with the H curve but with curves 1 or 2, or more accurately with their experimental analogs. In Fig. 5 the curves 1, 2, and M corresponding to laboratory conditions have been cut off at $J=0.7$, since for higher J cavities are usually recorded on the blades of the model later than in the vortices.

The third error is associated with the unsteadiness of the flow impinging on the blades and, on the basis of the results presented above, it can be stated that for large loads and small J this error will be small. The situation is different close to the design regime: curve 4 represents the result of the calculations for the blade of a propeller with $D=3.7$ m in the above-mentioned natural flow; in the calculations the values of J for this propeller were constructed using V^* . The values of J constructed from V^* are greater than 0.7 for real propeller operating regimes. Whereas when $J < 0.75$ curves 3 and 4 almost coincide, when $J > 0.9$ for the natural flow the theory proposed predicts the onset of cavitation no longer on the suction but on the pressure side of the blade, which is also responsible for the sharp bend in curve 4. Only with increase in the ratio of n to the speed of the vessel is it possible for cavitation to develop in the same form as under model conditions, i.e., on the suction side. The point in Fig. 5 represents the experimental value of σ_i under natural conditions.

Thus, in the quasisteady approach the critical cavitation numbers of the propellers may be considerably underestimated, and the predicted critical speed of the vessel may be unjustifiably high, especially for near-design regimes. This result points, in particular, to the need to take a cautious approach to the optimization of blade sections, for which methods developed for steady flow are currently being used (see, for example, [12, 13]). In view of the persisting difficulties in extrapolating the experimental data it is preferable to carry out a theoretical cavitation analysis even after the initial unsteady problem has been substantially simplified as proposed. However, it should be stressed that, like all such methods, the method of reducing the three-dimensional problem to a two-dimensional one described above is not universal.

The authors are grateful to S. V. Kaprantsev for assisting with the experiments.

REFERENCES

1. *Manual of Shipbuilding Theory*, Vol. 1 [in Russian], Sudostroenie, Leningrad (1985).
2. É. L. Amromin, V. G. Mishkevich, and K. V. Rozhdestvenskii, "Approximate calculation of three-dimensional cavitating flow around propeller blades in a viscous capillary fluid," *Izv. Akad. Nauk SSSR, Mekh. Zhidk. Gaza*, No. 6, 83 (1990).
3. *Marine Propellers. Modern Methods of Calculation* [in Russian], Sudostroenie, Leningrad (1983).
4. J. Hadamard, *Lectures on Cauchy's Problem in Linear Partial Differential Equations*, University Press, Paris (1922).
5. A. P. Mel'nikov, "The vortex method and its application to the construction of the potential flow over an airfoil," *Tr. Leningr. Voenno-Vozdush. Inzh. Akad.*, No. 27, 13 (1949).
6. N. E. Kochin, I. A. Kibel', and N. V. Roze, *Theoretical Hydromechanics*, Pt. 1 [in Russian], Fizmatgiz, Moscow (1963).
7. É. L. Amromin, A. V. Vasil'ev, and E. Ya. Semionicheva, "Problems of finding profiles with minimum critical cavitation number," *Zh. Prikl. Mekh. Tekh. Fiz.*, No. 5, 47 (1991).
8. É. L. Amromin, A. V. Vasil'ev, and V. V. Droblenkov, "Various approximations in the theory of viscous capillary cavitation flows," *Zh. Prikl. Mekh. Tekh. Fiz.*, No. 6, 117 (1988).
9. I. S. Pearsall, *Cavitation*, Mills and Boon, London (1972).
10. J. H. J. Van der Meulen, "Boundary layer and cavitation studies of NACA 16-012 and NACA 4412. Hydrofoils," *Proc. of the 13th Symp. on Naval Hydrodyn., Tokyo, 1980*, Tokyo (1981), p. 195.
11. É. L. Amromin, K. V. Aleksandrov, and Yu. L. Levkovskii, "Determination of the conditions of onset of cavitation on bodies with boundary-layer separation and reattachment," *Zh. Prikl. Mekh. Tekh. Fiz.*, No. 2, 34 (1986).
12. Y. T. Shen and R. Eppler, "Wing sections for hydrofoils," *J. Ship Res.*, **25**, 191 (1981).
13. A. M. Elizarov and D. A. Fokin, "Design of airfoils non-stall-free on a given range of angles of attack," *Izv. Akad. Nauk SSSR, Mekh. Zhidk. Gaza*, No. 3, 157 (1990).